Supplemental Information for

“High energy density polymeric nitrogen inside carbon nanotubes”

Chi Ding(丁驰)[1], Junjie Wang(王俊杰)[1], Yu Han(韩瑜)[1], Jianan Yuan(袁嘉男)[1],

Hao Gao(高豪)[1], and Jian Sun(孙建)[1,*]

[1]*National Laboratory of Solid State Microstructures,*

School of Physics and Collaborative Innovation Center of Advanced Microstructures,

Nanjing University, Nanjing, 210093, China

Contents

I. Structure search and implicit confining potentials;

II. Additional polymeric structures identified in our work;

III. Enthalpy results;

IV. Phonon spectrum and AIMD simulation results;

V. The size effects of carbon nanotubes on the structure of polymeric nitrogen;

VI. The temperature effects on the combined systems;

VII. Electronic properties;

VIII. Illustration of the energy density calculation;

IX. Coordinates for several of the typical structures.

* Corresponding author. jiansun@nju.edu.cn

I. Structure search and implicit confining potentials

In this article, we developed a new scheme of crystal structure searching in a confined space and employed it to predict polymeric nitrogen structures inside carbon nanotubes. The initial cells were set to be tetragonal with the cell parameters in *a*, *b* directions being 15 Å, and the length of the *c* axis being generated randomly. Because the confining potentials were in the *a*, *b* plane, the initial one-dimensional nitrogen structures were set to be in the *c* axis and it is periodic along this direction, the vacuum space in the *a*, *b* directions are larger than 10 Å between adjacent nitrogen polymers. There are 8, 10, 12, 16, 20, 24 nitrogen atoms in the cell respectively for every search. The external pressure was applied only along the *c* direction and the vertical pressure is defined as the uniaxial stress: $P = \sigma_{zz}$. The uniaxial stress is not conserved with varying bottom surface area[1]. The conserved quantities are the forces acting on the bottom surface: $F_z = \sigma_{zz}^{'} \cdot S^{'}$, where $S^{'}$ is the bottom surface area and $\sigma_{zz}^{'}$ is the calculated uniaxial stress[1]. In practical CNT bundles, the CNTs take the close-packed hexagonal configuration with the bottom surface area *S*. Because the polymeric nitrogen is finally loaded into the CNT bundles, the uniaxial stress for the quasi-1D polymeric nitrogen can be defined as $\sigma_{zz} = F_z/S$. In the structure optimization, we fixed the cell parameters in the *a*, *b* directions and only optimize the *c* axis until the vertical stress tensor converged to a target pressure. To make a thorough search for polymeric nitrogen phases inside CNTs, systematic crystal structure searches were performed for cells containing up to 24 nitrogen atoms with vertical pressures of 0, 2, 5, and 10 GPa.

To reduce the computational cost during the structure searching, external cylindrical confining potentials were introduced to represent the corresponding carbon nanotubes. We first calculated the binding energy of CNT and a nitrogen molecule versus their distance. Two different nitrogen configurations with the nitrogen molecule perpendicular and parallel to the *c* axis of the carbon nanotube were taken into consideration, they give very similar results. We also took into considerations of several van der walls interactions such as DFT-D3[2] and PBE+optB86b[3], they have little influence on the small size of CNTs. If not specified, we take the results from the parallel configuration with the optB86b functional in the following enthalpy calculations. These calculated results were well fitted to a Lennard-Jones type analytical potential $V(\mathrm{r}) = D \cdot \left(\left(\frac{k}{r+a}\right)^{12} - \left(\frac{k}{r+a}\right)^{6} +\right.$

$\left(\frac{k}{r-a}\right)^{12} - \left(\frac{k}{r-a}\right)^{6}\right)$, where r represent the distance between the center of nitrogen molecule and the center of CNTs. The calculated and fitted energy profiles for the (10, 0) CNT were plotted in Fig. S1(c), and the corresponding parameters of D, k and a for different carbon nanotubes were shown in Table. S1.

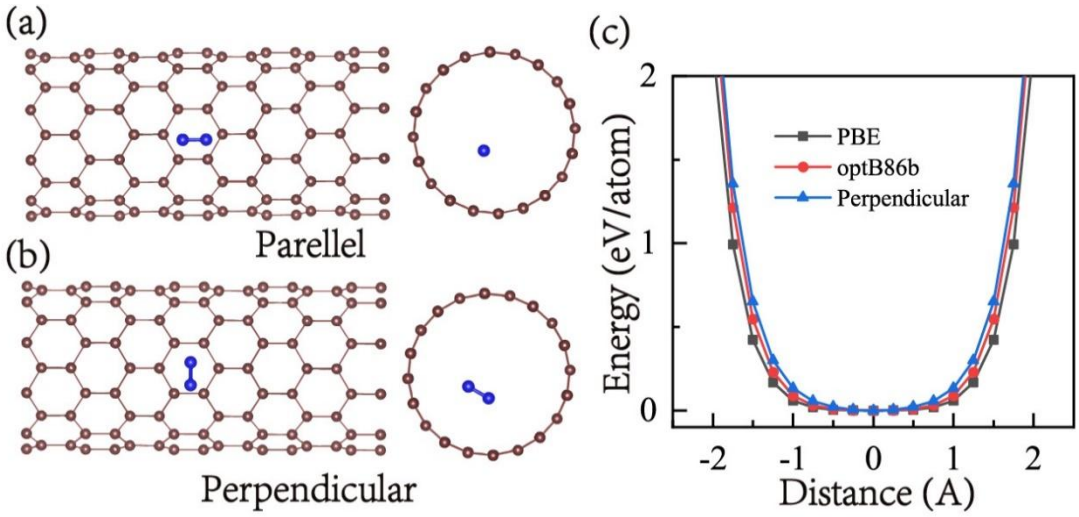

Figure S1. The Parallel (a) and Perpendicular (b) orientation of nitrogen unit in a typical (10, 0) carbon nanotube. (c) Calculated confining potentials of the parallel configuration with the PBE and optB86b functional, and of the perpendicular configuration.

Table S1. The diameters *d* of corresponding CNTs and the calculated parameters of *D*, *k* and *a* fitted to the energy profiles between nitrogen and CNTs.

	(5, 5)	(6, 6)	(7, 7)	(8, 0)	(9, 0)	(10, 0)	(11, 0)	(12, 0)
d /Å	6.78	8.14	9.49	6.26	7.05	7.83	8.61	9.39
D	24.3	1.49	0.8	23.0	8.45	7.56	1.10	0.85
k	8.68	6.13	5.66	8.33	7.30	7.62	5.92	5.77
a	10.6	7.70	7.77	9.96	8.92	9.59	7.67	7.83

II. Additional polymeric structures identified in our work;

There are several other types of polymeric nitrogen phases identified in our research work. Except for the one single polymeric nitrogen structure, several chains can be encapsulated together in one single cylindrical carbon nanotube. For example, two of the proposed ZZ1' phase can be loaded into the (n, 0) CNT as presented in Fig. S2 (a). These two chains are parallel to each other with the extra nitrogen atom in the opposite side of the zigzag chains. Three enhanced armchair chains can be confined in the (6, 6) CNT with a triangular configuration as shown in Fig. S2 (b). There are three steps in the enhanced armchair chain as denoted with the number, which is different from the normal armchair chain with two steps. This system is also what we obtained in the AIMD simulations when the AC3 were encapsulated into the much larger size of (6, 6) CNT. In addition, Fig. S2 (c) displayed a square nitrogen nanotube achieved in the (11, 0) CNT. The nitrogen polymer were composed of four zigzag chains the same as in the ZZ4 structure, but these chains are linked by one extra nitrogen atom instead of covalently bonded with each other directly. More interestingly, the four extra atoms linking every two zigzag chains as denoted with 1-4 are not in the same plane perpendicular to *c* axis, instead they form a helical structural along c axis. These three polymeric nitrogen structures were named as ZZ4', 2ZZ1' and 3eAC.

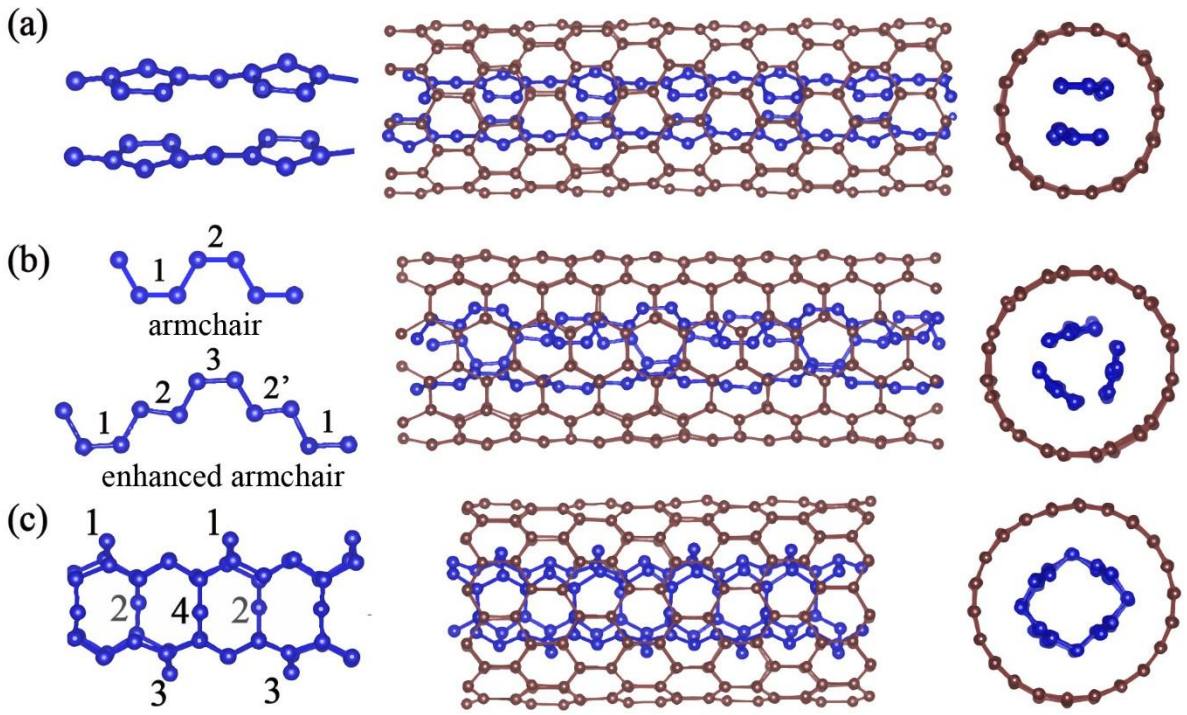

Figure S2. The Top and side view of three structures 2ZZ1', 3eAC and ZZ4' confined in (10, 0), (11, 0) and (6, 6) carbon nanotubes after AIMD simulations at 300K.

III. Enthalpy results

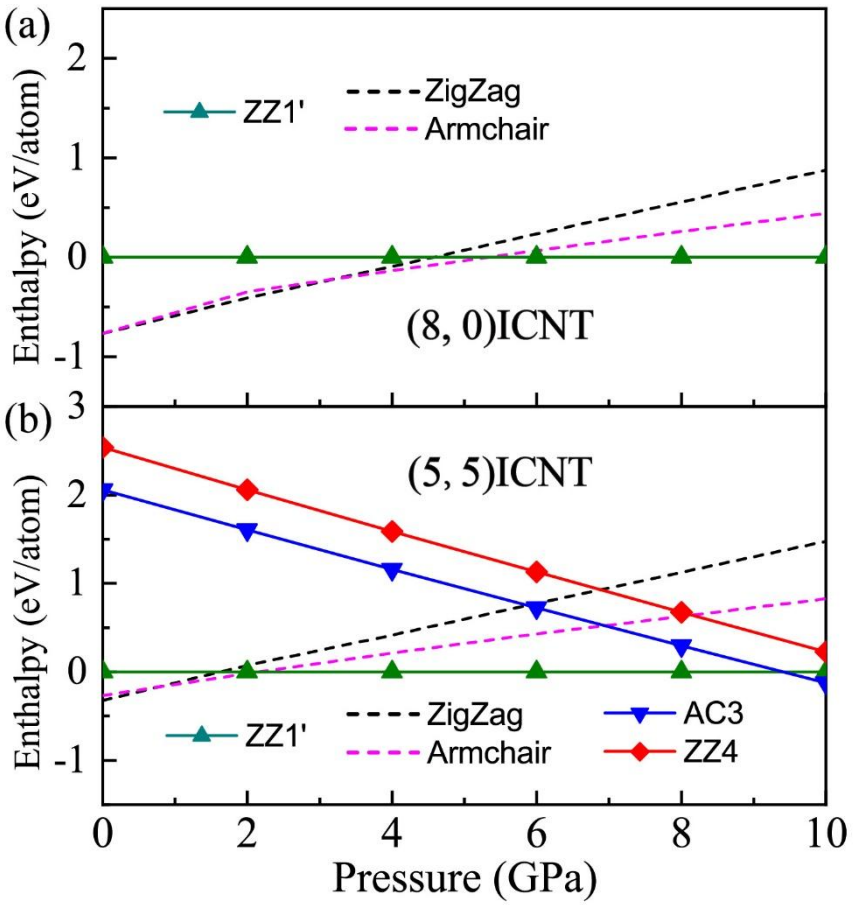

Figure S3. The enthalpy results of polymeric nitrogen structures confined within (a) (8, 0) ICNT and (b) (5, 5) ICNT. Because the (8, 0) CNT has a very small diameter of 6.26 Å, it can only accommodate the chain like polymeric structures, thus only the results for ZZ1', Zigzag and Armchair phases are presented

IV. Phonon spectra and AIMD simulation results

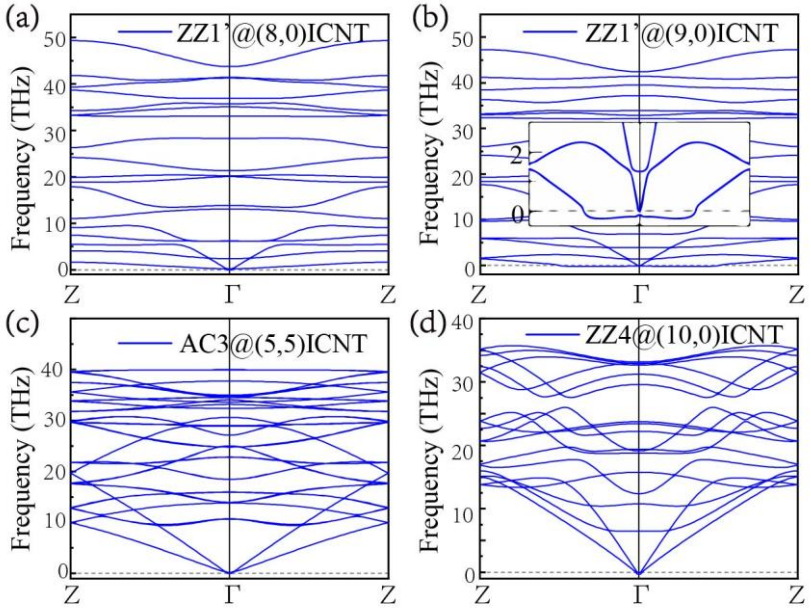

Figure S4. Phonon dispersive curves for ZZ1'@(8,0)ICNT, ZZ1'@(9,0)ICNT, AC3@(5,5)ICNT and ZZ4@(10,0)CNT at ambient vertical pressure.

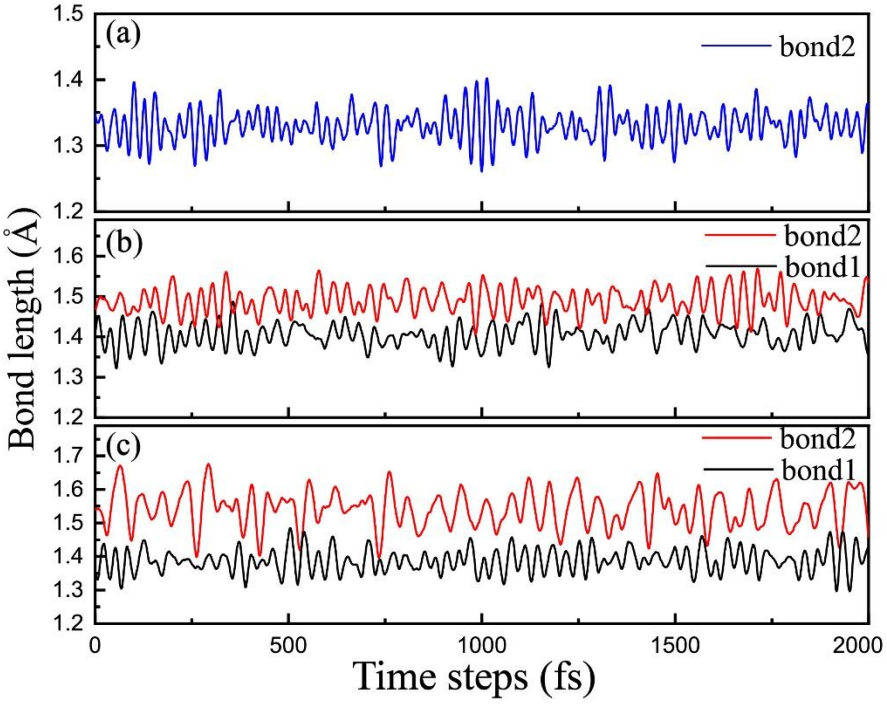

Figure S5. The evolution of bond length in the final 2000fs of three typical phases (a) ZZ1'@(9,0)CNT at 300K, (b)AC3@(5,5)CNT at 200K and (c) ZZ4@(10,0)CNT) at 300K.

V. The size effect of carbon nanotubes on the structure of polymeric nitrogen

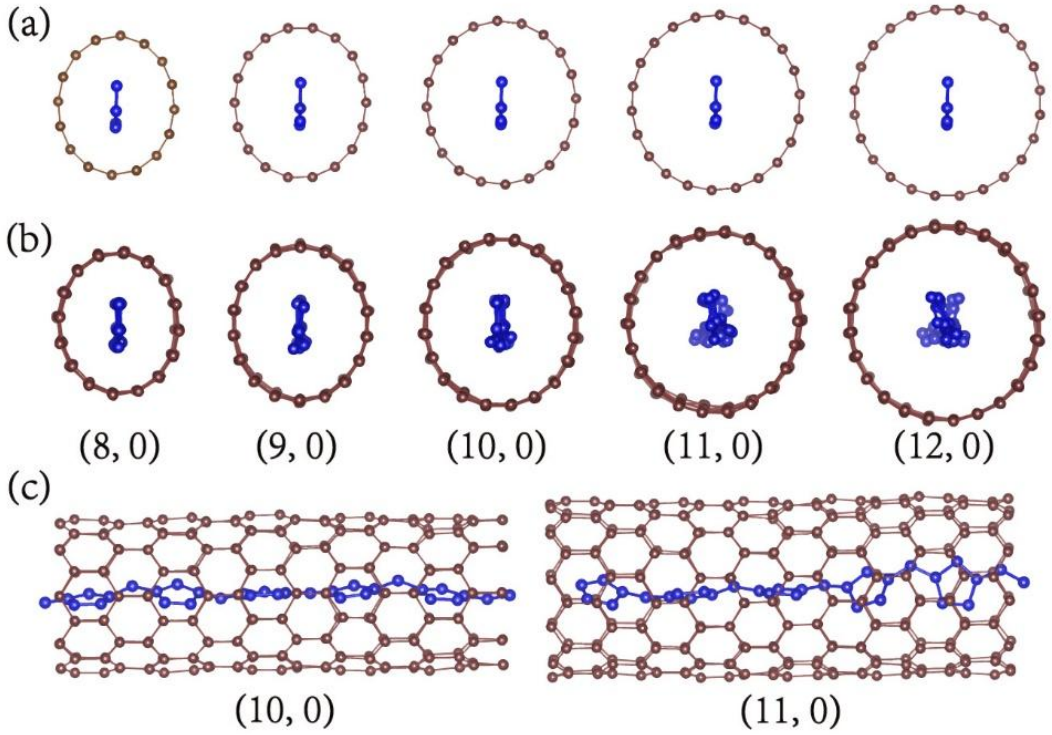

Figure S6. Polymeric ZZ1' nitrogen confined in different size of carbon nanotubes. The top view of these structures after geometry optimization (a) and after MD simulation (b) at 300K. (c) The side view of two typical systems with few and much twist after MD simulation.

Table S2. Four different bond length (d1, d2, d3 and d4) of polymeric ZZ1' phase confined in (n, 0) CNT with n=8-12. The semi-major (a) and semi-minor (b) axis of the fully optimized elliptical carbon nanotubes, their deformation ratio (δ_{ab}) and the radius of the origin circular CNTs (R0).

	a	b	δ_{ab}	R0	d1	d2	d3	d4	average
(8, 0)	3.509	2.927	19.9%	3.166	1.316	1.322	1.318	1.324	1.320
(9, 0)	3.757	3.316	13.3%	3.527	1.327	1.329	1.338	1.331	1.331
(10, 0)	4.122	3.766	9.4%	3.985	1.331	1.331	1.348	1.331	1.335
(11, 0)	4.421	4.233	4.4%	4.379	1.332	1.333	1.351	1.331	1.337
(12, 0)	4.685	4.674	0.2%	4.685	1.333	1.333	1.353	1.331	1.338

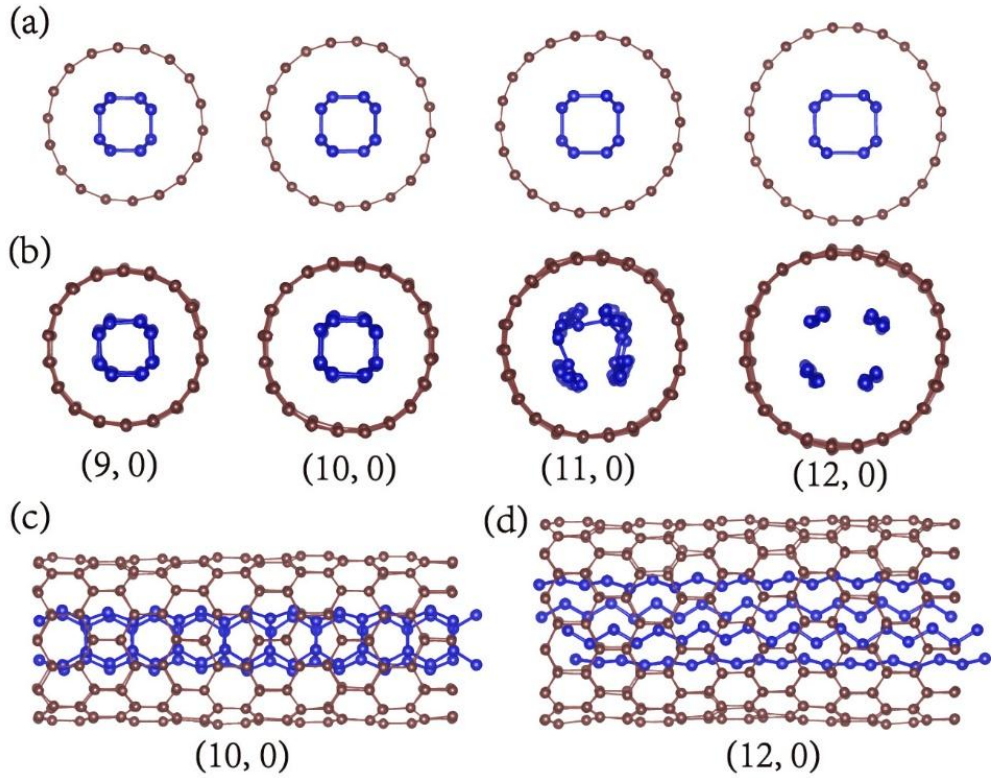

Figure S7. Polymeric ZZ4 nitrogen nanotube confined in different size of carbon nanotubes. The top view of these structures after geometry optimization (a) and after MD simulation at 300K (b). The side view of two typical systems confined in (10, 0) CNT (c) and (12, 0) CNT (d) after MD simulations.

Table S3. Calculated lattice parameter of ZZ4@(n,0)CNT (n=9-11). Including the radius of CNT before and after encapsulated with nitrogen (R0 and R), their deformation ratio (δ_R) and the bond-length of N-N (d1 and d2).

	R0	R	δ_R	d1	d2
(9, 0)	3.538	3.789	7.1%	1.367	1.465
(10, 0)	3.920	4.096	4.5%	1.379	1.525
(11, 0)	4.312	4.384	1.7%	1.384	1.606

VI. The temperature effects on the combined systems

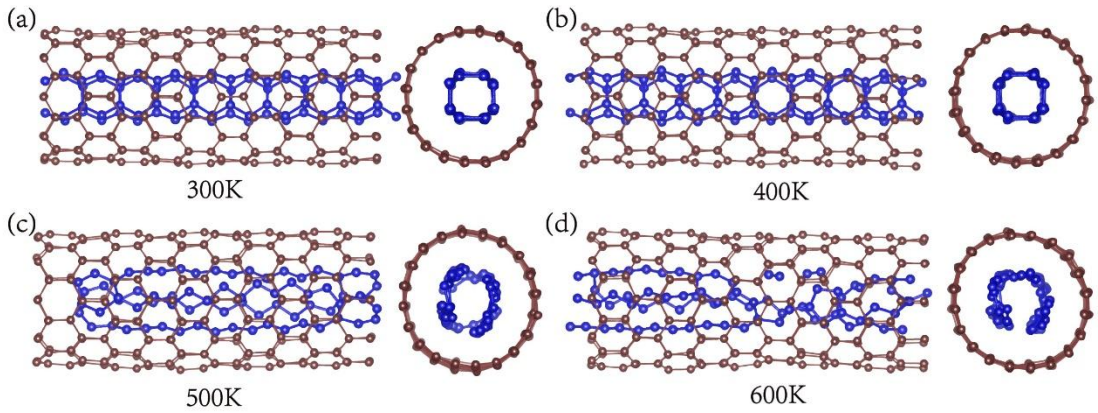

Figure S8. Polymeric ZZ4 nitrogen nanotube confined in (10,0)CNT at different temperatures from 300K to 600K.

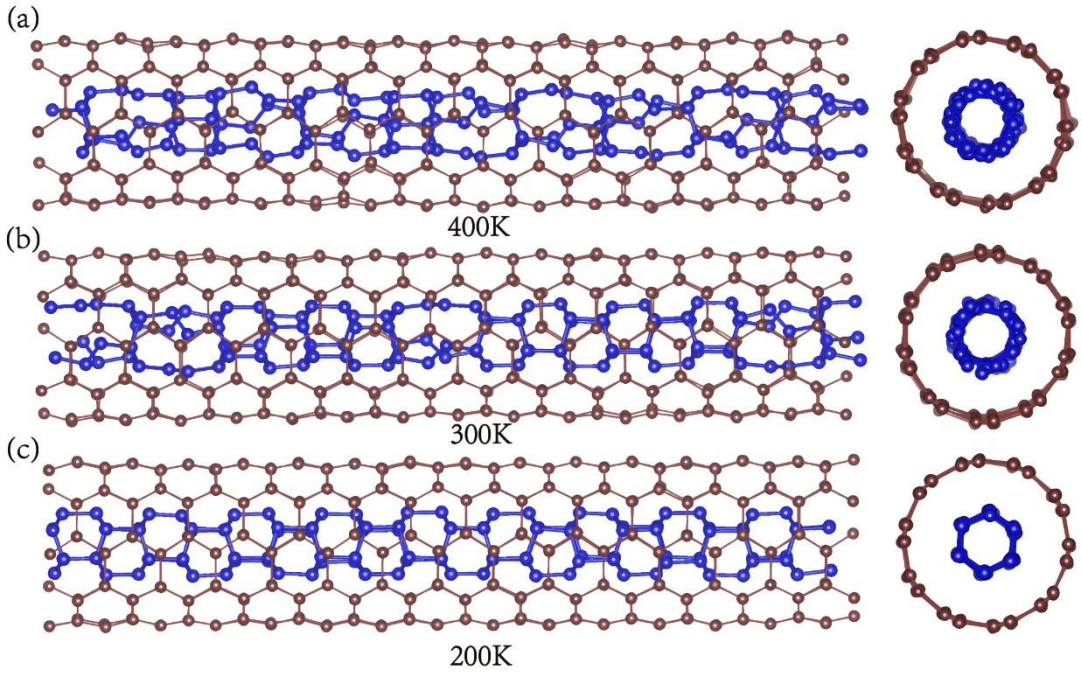

Figure S9. Structures of AC3 confined in (5,5) CNT after MD simulations at temperatures from 200K to 400K. The optimized radius of isolated (5, 5) CNT at 0K is about 3.4 Å, which expands to 3.65 Å after the filling of polymeric nitrogen AC3, the corresponding deformation ratio of CNT is about 7.35%.

VII. Electronic properties

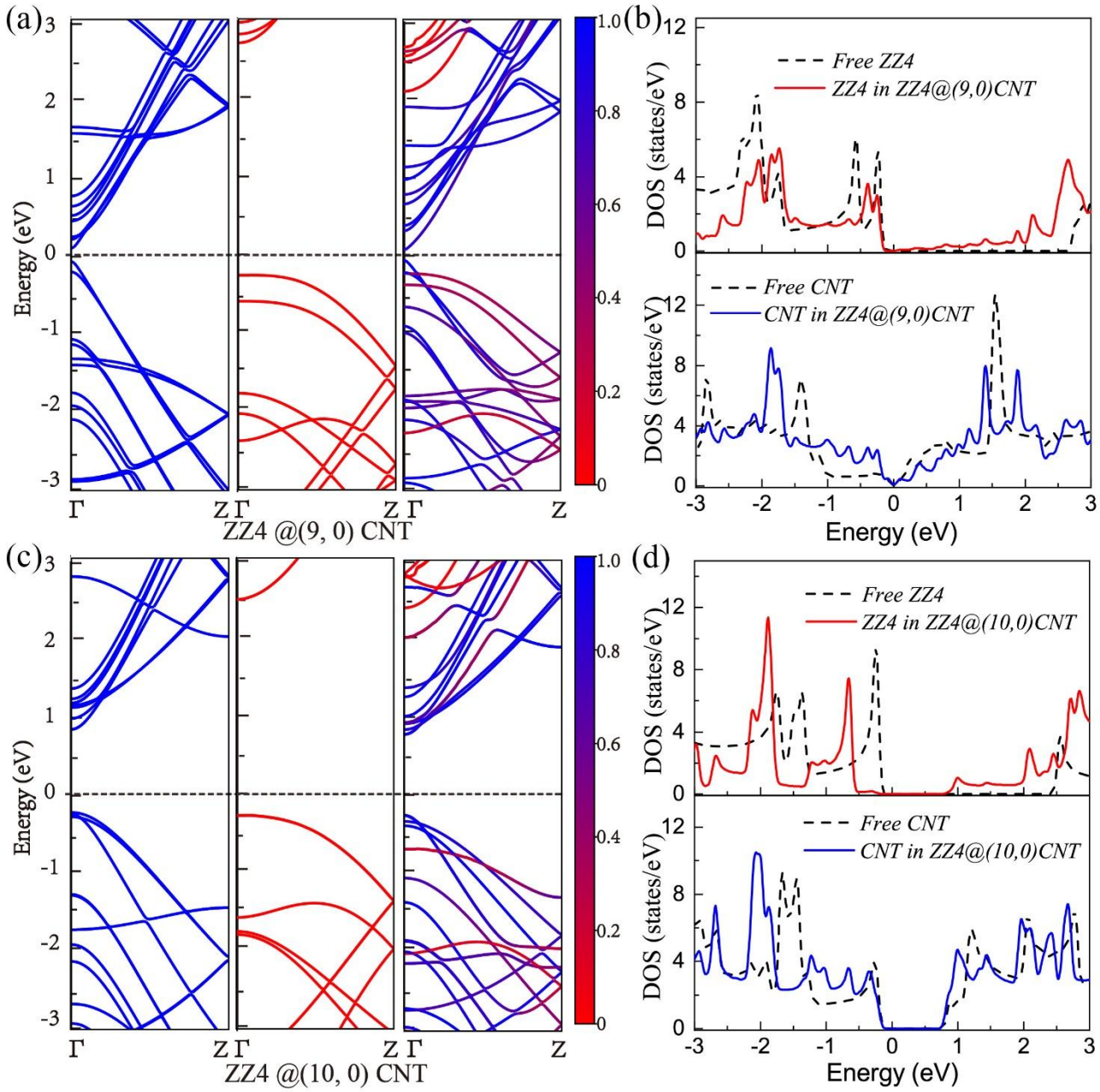

Figure S10. The electronic properties of ZZ4 confined in (9,0) and (10,0)CNT respectively.

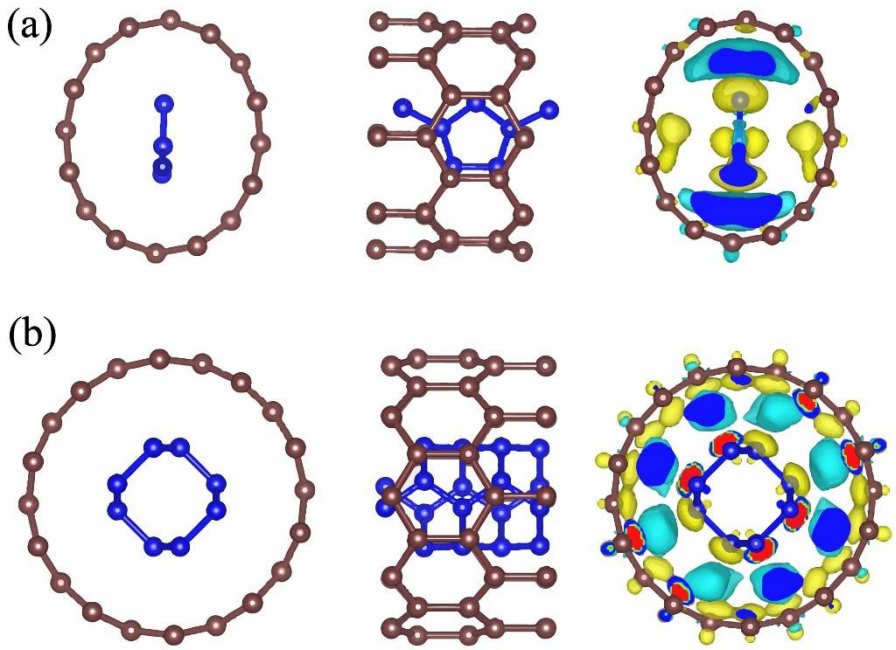

Figure S11. Top and side view of the optimized structures of two combined systems: (a) ZZ1'@(8,0)CNT and (b) ZZ4@(10,0)CNT, and the charge density difference between the combined systems and the sum of stand-alone nitrogen and carbon nanotube with the isosurface values $0.8\text{x}10^{-3}$ and $0.9\text{x}10^{-3}$ respectively.

VIII. Illustration of the energy density calculation

We calculated the gravimetric energy density of these combined systems with the following formula:

$$E_d = [E_{combined} - E_{CNT} - (E_{\alpha-N} - 0.25) * N]/M$$

and then the volumeric energy density is calculated with $E_v = E_d * M/V$. In the formula above, $E_{combined}$ and E_{CNT} represents the energy of the combined systems and the fully optimized carbon nanotube after removing polymeric nitrogen, respectively. *N* is the number of nitrogen atoms, *M* represents the mass of the combined systems, *V* are taken as the volume of corresponding carbon nanotube bundles with a hexgonal lattice. The number "0.25" in above formula represents the reduction of the free energy from the molecular crystal α-N to nitrogen gas[4].

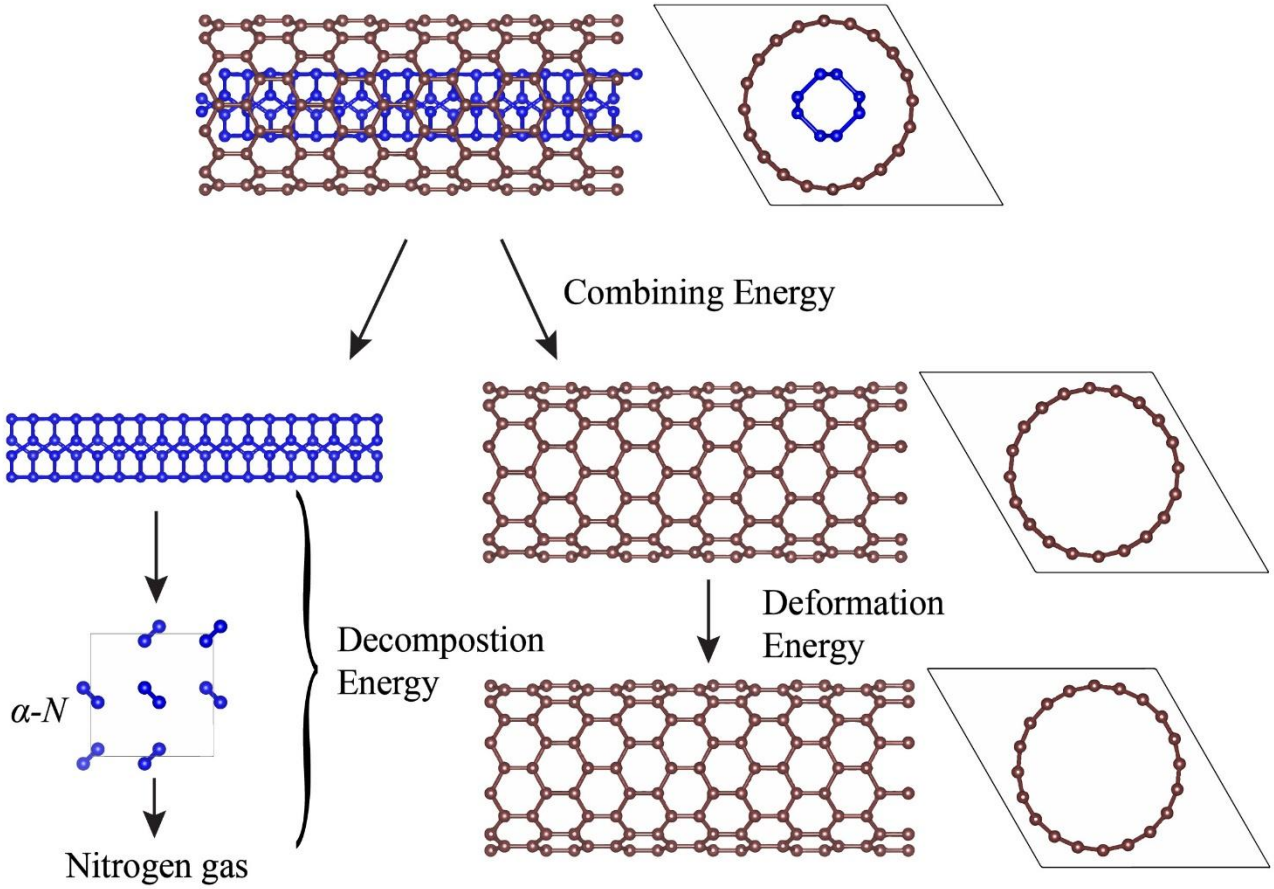

Figure S12. Illustration of the total and parts of the energy density calculations.

Table. S4. The density (ρ), gravimetric (E_d) and volumetric (E_v) energy density of these combined systems compared to the experiment results of the known TNT explosive. The total energy densities are composed by three parts, the decomposition energy (E_1) from polymeric nitrogen to isolated molecules, the deformation energy (E_2) of CNT and the combining energy (E_3) between the polymeric nitrogen and carbon nanotube.

Systems	ρ (g/cm^{-3})	$E_d(kJ/g)$	$E_v(kJ/cm^{-3})$	E_1 (kJ/g)	E_2 (kJ/g)	E_3 (kJ/g)
zigzag@(9,0)CNT	2.02	0.98	1.99	1.328	0.004	-0.349
armchair@(5,5)CNT	2.04	1.41	2.87	1.555	0.012	-0.161
ZZ1'@(9,0)CNT	2.10	1.88	3.95	1.878	0.038	-0.031
ZZ1'@(8,0)CNT	2.16	2.68	5.80	2.090	0.122	0.469
AC3@(5,5)CNT	2.37	7.46	17.68	5.267	0.787	1.405
ZZ4@(9,0)CNT	2.38	7.49	17.78	5.382	0.781	1.322
ZZ4@(10,0)CNT	2.40	5.34	12.80	4.654	0.204	0.482
TNT	1.64	4.30	7.05			

IX. Coordinates for several of the typical structures

Here we present the coordinates for three typical structures of polymeric nitrogen optimized in corresponding implicit carbon nanotubes ZZ1'@(9,0)ICNT (data_1), AC3@ (5,5)ICNT (data_2) and ZZ4@(10, 0)ICNT (data_3). The coordinates for three additional nitrogen structures displayed above 2ZZ1' @(10, 0)ICNT (data_4), ZZ4' @ (11, 0)ICNT (data_5) and 3eAC@(6, 6)ICNT (data_6) are also provided.

```
data_1


_chemical_name_common                  'N                                        '
_cell_length_a                         15.00000
_cell_length_b                         15.00000
_cell_length_c                         4.38340
_cell_angle_alpha                      90
_cell_angle_beta                       90
_cell_angle_gamma                      90
_space_group_name_H-M_alt              'P 1'
_space_group_IT_number                 1

loop_
_space_group_symop_operation_xyz
   'x, y, z'

loop_
   _atom_site_label
   _atom_site_occupancy
   _atom_site_fract_x
   _atom_site_fract_y
   _atom_site_fract_z
   _atom_site_adp_type
   _atom_site_B_iso_or_equiv
   _atom_site_type_symbol
   N1         1.0     0.501116      0.567202      0.649018     Biso  1.000000 N
   N2         1.0     0.501116      0.567201      0.345432     Biso  1.000000 N
   N3         1.0     0.500285      0.427548      0.497237     Biso  1.000000 N
   N4         1.0     0.496685      0.440208      0.997233     Biso  1.000000 N
   N5         1.0     0.500142      0.482500      0.732849     Biso  1.000000 N
   N6         1.0     0.500142      0.482496      0.261617     Biso  1.000000 N
```

data_2

```
_chemical_name_common                  'N                                        '
_cell_length_a                         15.00000
_cell_length_b                         15.00000
_cell_length_c                         3.83403
_cell_angle_alpha                      90
_cell_angle_beta                       90
_cell_angle_gamma                      90
_space_group_name_H-M_alt              'P 1'
_space_group_IT_number                 1

loop_
_space_group_symop_operation_xyz
   'x, y, z'

loop_
   _atom_site_label
   _atom_site_occupancy
   _atom_site_fract_x
   _atom_site_fract_y
   _atom_site_fract_z
   _atom_site_adp_type
   _atom_site_B_iso_or_equiv
   _atom_site_type_symbol
   N1         1.0     0.414851      0.498548      0.055927     Biso  1.000000 N
   N2         1.0     0.414851      0.498548      0.444073     Biso  1.000000 N
   N3         1.0     0.541330      0.574461      0.055917     Biso  1.000000 N
   N4         1.0     0.541330      0.574461      0.444083     Biso  1.000000 N
   N5         1.0     0.458674      0.425524      0.944081     Biso  1.000000 N
   N6         1.0     0.585152      0.501436      0.944073     Biso  1.000000 N
   N7         1.0     0.543831      0.426967      0.055921     Biso  1.000000 N
   N8         1.0     0.456171      0.573018      0.944080     Biso  1.000000 N
   N9         1.0     0.543831      0.426967      0.444079     Biso  1.000000 N
   N10        1.0     0.456171      0.573018      0.555920     Biso  1.000000 N
   N11        1.0     0.458674      0.425524      0.555919     Biso  1.000000 N
   N12        1.0     0.585152      0.501436      0.555927     Biso  1.000000 N
```

```
data_3


_chemical_name_common                  'N                                        '
_cell_length_a                         15.00000
_cell_length_b                         15.00000
_cell_length_c                         2.27347
_cell_angle_alpha                      90
_cell_angle_beta                       90
_cell_angle_gamma                      90
_space_group_name_H-M_alt              'P 1'
_space_group_IT_number                 1

loop_
_space_group_symop_operation_xyz
   'x, y, z'

loop_
   _atom_site_label
   _atom_site_occupancy
   _atom_site_fract_x
   _atom_site_fract_y
   _atom_site_fract_z
   _atom_site_adp_type
   _atom_site_B_iso_or_equiv
   _atom_site_type_symbol
   N1         1.0     0.596085      0.474107      0.500000     Biso  1.000000 N
   N2         1.0     0.403915      0.525893      0.500000     Biso  1.000000 N
   N3         1.0     0.525894      0.596086      0.000000     Biso  1.000000 N
   N4         1.0     0.474106      0.403914      1.000000     Biso  1.000000 N
   N5         1.0     0.403914      0.474106      1.000000     Biso  1.000000 N
   N6         1.0     0.596086      0.525894     -0.000000     Biso  1.000000 N
   N7         1.0     0.474107      0.596085      0.500000     Biso  1.000000 N
   N8         1.0     0.525893      0.403915      0.500000     Biso  1.000000 N
```

```
data_4

_chemical_name_common                  'N                                   '
_cell_length_a                         20.00000
_cell_length_b                         20.00000
_cell_length_c                         4.37808
_cell_angle_alpha                      90
_cell_angle_beta                       90
_cell_angle_gamma                      90
_space_group_name_H-M_alt              'P 1'
_space_group_IT_number                 1

loop_
_space_group_symop_operation_xyz
   'x, y, z'

loop_
   _atom_site_label
   _atom_site_occupancy
   _atom_site_fract_x
   _atom_site_fract_y
   _atom_site_fract_z
   _atom_site_adp_type
   _atom_site_B_iso_or_equiv
   _atom_site_type_symbol
   N1         1.0     0.559532      0.518421      0.736309     Biso  1.000000 N
   N2         1.0     0.440468      0.481579      0.263691     Biso  1.000000 N
   N3         1.0     0.440468      0.481579      0.736309     Biso  1.000000 N
   N4         1.0     0.559532      0.518421      0.263691     Biso  1.000000 N
   N5         1.0     0.562613      0.454330      0.650007     Biso  1.000000 N
   N6         1.0     0.437387      0.545670      0.349993     Biso  1.000000 N
   N7         1.0     0.437387      0.545670      0.650007     Biso  1.000000 N
   N8         1.0     0.562613      0.454330      0.349993     Biso  1.000000 N
   N9         1.0     0.443886      0.440807      0.500000     Biso  1.000000 N
   N10        1.0     0.556114      0.559193      0.500000     Biso  1.000000 N
   N11        1.0     0.456105      0.452007     -0.000000     Biso  1.000000 N
   N12        1.0     0.543895      0.547993      0.000000     Biso  1.000000 N
```

```
data_5


_chemical_name_common                  'N                                   '
_cell_length_a                         20.00000
_cell_length_b                         20.00000
_cell_length_c                         4.48880
_cell_angle_alpha                      90
_cell_angle_beta                       90
_cell_angle_gamma                      90
_space_group_name_H-M_alt              'P 1'
_space_group_IT_number                 1

loop_
_space_group_symop_operation_xyz
   'x, y, z'

loop_
   _atom_site_label
   _atom_site_occupancy
   _atom_site_fract_x
   _atom_site_fract_y
   _atom_site_fract_z
   _atom_site_adp_type
   _atom_site_B_iso_or_equiv
   _atom_site_type_symbol
   N1         1.0     0.547847      0.582274      0.583549     Biso  1.000000 N
   N2         1.0     0.452152      0.417728      0.083552     Biso  1.000000 N
   N3         1.0     0.417729      0.547848      0.333554     Biso  1.000000 N
   N4         1.0     0.582272      0.452154      0.833547     Biso  1.000000 N
   N5         1.0     0.442904      0.576163      0.568438     Biso  1.000000 N
   N6         1.0     0.557098      0.423839      0.068435     Biso  1.000000 N
   N7         1.0     0.423838      0.442902      0.318439     Biso  1.000000 N
   N8         1.0     0.576162      0.557099      0.818441     Biso  1.000000 N
   N9         1.0     0.452669      0.422227      0.566795     Biso  1.000000 N
   N10        1.0     0.547333      0.577774      0.066789     Biso  1.000000 N
   N11        1.0     0.577772      0.452670      0.316791     Biso  1.000000 N
   N12        1.0     0.422230      0.547330      0.816794     Biso  1.000000 N
   N13        1.0     0.555981      0.428351      0.585191     Biso  1.000000 N
   N14        1.0     0.444021      0.571651      0.085194     Biso  1.000000 N
   N15        1.0     0.571651      0.555980      0.335190     Biso  1.000000 N
   N16        1.0     0.428349      0.444019      0.835193     Biso  1.000000 N
   N17        1.0     0.387346      0.493428      0.825989     Biso  1.000000 N
   N18        1.0     0.612654      0.506575      0.325986     Biso  1.000000 N
```

```
   N19         1.0      0.506573      0.387346      0.575986     Biso  1.000000 N
   N20         1.0      0.493427      0.612657      0.075986     Biso  1.000000 N
```

data_6

```
_chemical_name_common                  'N                                   '
_cell_length_a                         20.00000
_cell_length_b                         20.00000
_cell_length_c                         8.15994
_cell_angle_alpha                      90
_cell_angle_beta                       90
_cell_angle_gamma                      90
_space_group_name_H-M_alt              'P 1'
_space_group_IT_number                 1

loop_
_space_group_symop_operation_xyz
   'x, y, z'

loop_
   _atom_site_label
   _atom_site_occupancy
   _atom_site_fract_x
   _atom_site_fract_y
   _atom_site_fract_z
   _atom_site_adp_type
   _atom_site_B_iso_or_equiv
   _atom_site_type_symbol
   N1          1.0      0.578630      0.515645      0.172922     Biso  1.000000 N
   N2          1.0      0.515652      0.578640      0.827077     Biso  1.000000 N
   N3          1.0      0.515653      0.578639      0.672922     Biso  1.000000 N
   N4          1.0      0.578629      0.515647      0.327081     Biso  1.000000 N
   N5          1.0      0.423852      0.513669      0.077568     Biso  1.000000 N
   N6          1.0      0.513675      0.423841      0.922431     Biso  1.000000 N
   N7          1.0      0.513674      0.423840      0.577575     Biso  1.000000 N
   N8          1.0      0.423851      0.513669      0.422425     Biso  1.000000 N
   N9          1.0      0.560245      0.447252      0.672865     Biso  1.000000 N
   N10         1.0      0.447252      0.560251      0.327122     Biso  1.000000 N
   N11         1.0      0.447253      0.560253      0.172879     Biso  1.000000 N
   N12         1.0      0.560246      0.447253      0.827135     Biso  1.000000 N
```

N13	1.0	0.427427	0.526152	0.577556	Biso	1.000000 N
N14	1.0	0.526155	0.427429	0.422445	Biso	1.000000 N
N15	1.0	0.526154	0.427429	0.077555	Biso	1.000000 N
N16	1.0	0.427427	0.526151	0.922444	Biso	1.000000 N
N17	1.0	0.474115	0.424027	0.172856	Biso	1.000000 N
N18	1.0	0.424036	0.474108	0.827137	Biso	1.000000 N
N19	1.0	0.424036	0.474109	0.672857	Biso	1.000000 N
N20	1.0	0.474116	0.424027	0.327148	Biso	1.000000 N
N21	1.0	0.549876	0.559070	0.077559	Biso	1.000000 N
N22	1.0	0.559064	0.549863	0.922442	Biso	1.000000 N
N23	1.0	0.559065	0.549863	0.577562	Biso	1.000000 N
N24	1.0	0.549875	0.559071	0.422437	Biso	1.000000 N

References

[1] Chen J, Schusteritsch G, Pickard C J, Salzmann C G and Michaelides A 2016 *Phys. Rev. Lett.* **116** 025501.

[2] Grimme S, Antony J, Ehrlich S and Krieg H 2010 *The Journal of Chemical Physics* **132** 154104.

[3] Klimeš J, Bowler D R and Michaelides A 2009 *Journal of Physics: Condensed Matter* **22** 022201.

[4] Zhang J, Oganov A R, Li X and Niu H 2017 *Physical Review B* **95** 020103.